

# Dramatic Improvement of Stability by In-Situ Linker Cyclization of a Metal-Organic Framework

Yun-Long Hou<sup>†</sup>, Mu-Qing Li<sup>†‡§</sup>, Shengxian Cheng<sup>†</sup>, Yingxue Diao<sup>†§</sup>, Filipe Vilela<sup>||</sup>, Yonghe He<sup>⊥</sup>, Jun He<sup>⊥</sup> and Zhengtao Xu<sup>\*†</sup>

<sup>†</sup> Department of Chemistry, City University of Hong Kong, 83 Tat Chee Avenue, Kowloon, Hong Kong, China

<sup>‡</sup> Frontier Institute of Science and Technology, Xi'an Jiaotong University, Xi'an 710054, China

<sup>§</sup> Department of Material Science and Engineering, City University of Hong Kong, 83 Tat Chee Avenue, Kowloon, Hong Kong, China

<sup>||</sup> School of Engineering and Physical Sciences, Institute of Chemical Sciences, Heriot-Watt University, Edinburgh, UK

<sup>⊥</sup> School of Chemical Engineering and Light Industry, Guangdong University of Technology, Guangzhou 510006, China

## Supporting Information Placeholder

**ABSTRACT:** We employ a two-step strategy for accessing crystalline porous covalent networks of highly conjugated  $\pi$ -electron systems. For this, we first assembled a crystalline metal-organic framework (MOF) precursor based on Zr(IV) ions and a linear dicarboxyl linker molecule featuring backfolded, highly unsaturated alkyne backbones; massive thermocyclization of the organic linkers was then triggered to install highly conjugated, fused-aromatic bridges throughout the MOF scaffold while preserving the crystalline order. The formation of cyclized carbon links not only greatly strengthen the precursor coordination scaffold, but more importantly, enhance electroactivity and charge transport throughout the polycyclic aromatic grid.

The making of crystalline porous carbon networks (e.g., as the 3D analog of the 2D graphene system) is of interest in view of stability, functionality, and electronic/catalytic applications.<sup>1</sup> One prime example is the gyroid and other minimal surfaces (e.g., the Schwarz P and D surfaces) tiled with carbon polygons to generate 3D carbon schwarzites (or Mackay-Terrones crystals). Since the initial proposition in the 1990s,<sup>2</sup> theoretical studies have pointed to the intriguing electronic properties of these negatively curved carbon networks;<sup>3</sup> experimentally accessing these 3D carbon crystals, however, remains a challenge. One difficulty concerns the very strong constituent C-C bond that tends to form irreversibly and thereby disrupt the order of the forming network. This dilemma of crystallinity and bond strength is also conspicuous in the study of metal-organic<sup>4</sup> and covalent organic frameworks (MOF and COF).<sup>5</sup> Namely, their crystallinity critically depends on the reversible coordination interactions (e.g., metal-imidazolite and metal-carboxylate bonds) or covalent links (e.g., imine links from amino and carbonyl condensations), stronger links like C-C bonds and many metal-thiolate bonds often result in poor structural order.

In this regard, the two-step approach, which separates crystallization from covalent bond formation, proves widely effective for integrating strong covalent links into crystalline nets in a post-synthetic fashion.<sup>6</sup> Therein, a crystalline porous net is first assembled from metal ions and an organic linker with tailor-made side groups (e.g., thiol groups). A reactive agent (e.g., a metal guest of HgCl<sub>2</sub>)<sup>6c</sup> was then diffused into the coordination solid to install the covalent links (e.g., that of Hg-thiolate).

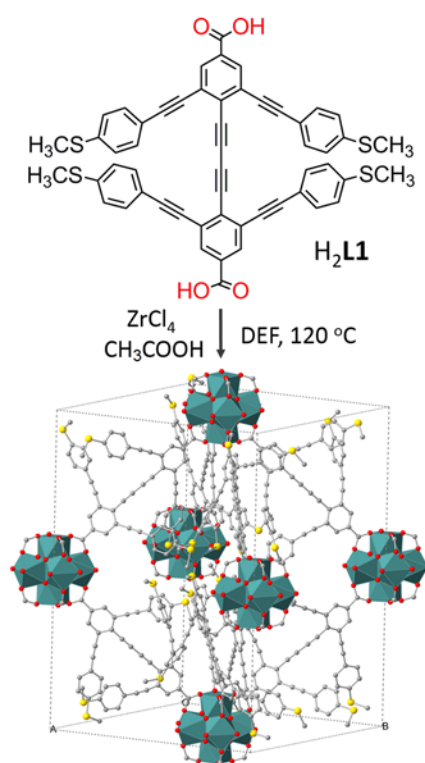


**Fig. 1.** Linker molecule H<sub>2</sub>L1 (featuring 4 backfolded alkyne backbones) reacts with ZrCl<sub>4</sub> to form the ZrL1 net (shown as an octahedroid based on Zr-O clusters and L1 linkers). ZrL1 topologically resembles the UiO series, but with four equatorial linkers absent in the octahedroid unit.

Herein we report a dramatic rendition of this powerful two-step synthesis, in the context of accessing highly stable and crystalline polycyclic aromatic networks. The key design builds on the symmetrically backfolded<sup>6d, 7</sup> linker L1 (Fig. 1; see also Fig. S1 for the synthetic steps): the dicarboxylic termini serve to establish the crystalline framework with Zr(IV) ions, while the unsaturated alkyne units subsequently thermocyclize to effect the transition into a more

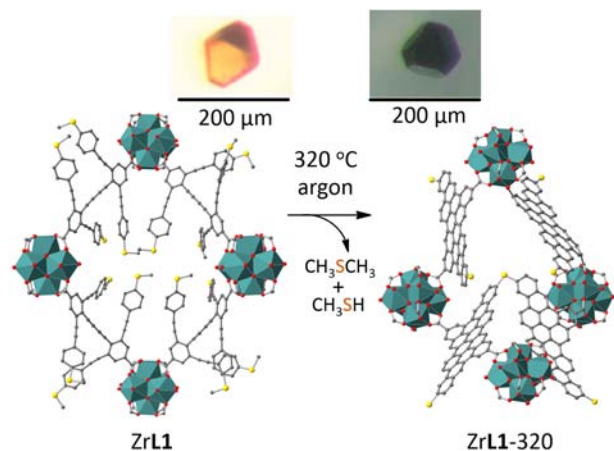


**Fig. 2.** Schematic of the thermally induced linker transformation of the ZrL1 crystal (structure represented by a quadrilateral aperture of the net). The resulted network (ZrL1-320; on the right) likely contains covalent links (e.g., the aryl-S-aryl unit) across the individual aromatic linkers. Zr atoms: cyan; S: orange; C: grey; O: red.

robust conjugated aromatic network (Fig. 2 and S8). Unlike the destructive, high-temperature (e.g., above 800 °C) carbonization of MOF solids,<sup>8</sup> the alkyne benzannulation here occurs at milder conditions (e.g., 200-400°C), preserving the crystallinity of the MOF scaffold, whilst accommodating richer functional design.

Solvothermally reacting L1 with ZrCl<sub>4</sub> in *N,N*-diethylformamide (DEF), using acetic acid as the modulator, afforded truncated octahedra of orange crystals (about 0.1 mm in size; see also Fig. 2 and S2 for a photograph of the crystal). Even though single crystal X-ray diffraction (SCXRD) analysis on

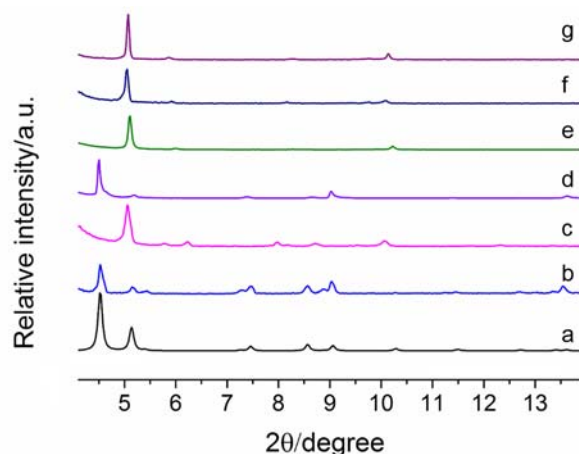


**Fig. 3.** PXRD patterns (Cu K $\alpha$ ,  $\lambda = 1.5418 \text{ \AA}$ ) for (a) a model based on Lin's tetragonal, 8-connected UiO-type MOF (ref. 9); (b) an as-made sample of ZrL1; (c) an activated sample of ZrL1 (in air), i.e., ZrL1-ac; (d) sample (c) immersed in DMF for 24 hours, i.e., ZrL1-DMFg; (e) sample (b) heated at 320 °C for 3 hours, i.e., ZrL1-320; (f) sample (e) immersed in a saturated (4% w/w) NaF solution (50 °C, 24 hours); (g) sample (e) immersed in H<sub>3</sub>PO<sub>4</sub> (10% w/w) for 24 hours.

the crystals has not been successful due to very weak diffraction observed (on a Bruker APEX diffractometer), powder X-ray diffraction reveals a tetragonal unit cell ( $a = 24.34$ ,  $c = 32.65 \text{ \AA}$ ; pattern b, Fig. 3; details of refinement also included in ESI). The formula Zr<sub>6</sub>O<sub>4</sub>(OH)<sub>8</sub>(H<sub>2</sub>O)<sub>4</sub>(L1)<sub>4</sub> for the activated crystal sample of ZrL1 is supported by elemental analysis and solution <sup>1</sup>H-NMR measurement (with the crystals dissolved in a DMSO-*d*<sub>6</sub>/K<sub>3</sub>PO<sub>4</sub>/D<sub>2</sub>O solution to indicate the structural intactness of the L1 linker; see Fig. S3). The 1:4 cluster/linker ratio in ZrL1 points to 8-connected Zr<sub>6</sub>O<sub>4</sub>(OH)<sub>8</sub>(H<sub>2</sub>O)<sub>4</sub> clusters; together with the tetragonal symmetry revealed by PXRD, the framework structure of ZrL1 can be compared to a tetragonal Zr-MOF reported by Lin's group<sup>9</sup> (e.g., see patterns a and b of Fig. 3, in which the Zr<sub>6</sub> cluster is 8-connected, with each octahedroid cage missing four equatorial linkers (Fig. 1, bottom). The missing equatorial edges provide structural flexibility, allowing the octahedron to be distorted normal to the basal plane, to give a tetragonal lattice. Thus ZrL1, with the 8-connected Zr-O cluster, adopts the **bcu** topology as compared with the **fcu** topology of the 12-connected prototype. Note that ZrL1 differs from the PCN-700 series,<sup>10</sup> which also features 8-connected nodes and a **bcu** topology. In ZrL1, all the Zr<sub>6</sub> octahedra are identically oriented, with their equatorial squares perpendicular to the *c* axis; in PCN-700, however, each two linker-sharing Zr<sub>6</sub> octahedra are related by the 4<sub>2</sub> axis; their equatorial bases, while both paralleling the *c* axis, are perpendicular to the *a* and *b* axis, respectively.

Distinct framework dynamics and flexibility of the ZrL1 network was revealed in X-ray diffraction studies. For example, the activated sample ZrL1-ac (the activation promotes the removal of the guest molecules) exhibits diffraction peaks (e.g., the dominant low angle peak; see pattern c, Fig. 3) that are significantly shifted to larger values (towards the right), indicating contraction of the host lattice. Upon immersion in DMF solvent, the peaks (pattern d, Fig. 3) are shifted back to the similar positions as in the pristine, as-made ZrL1 sample (see ESI for cell refinements).

One intriguing result arises from the thermal treatment of the ZrL1 crystals. For example, after heating at 320 °C for three hours under a flow of argon, the orange crystals turned black (Fig. S4), whilst retaining the highly crystalline lattice, as indicated by the sharp and strong PXRD peaks observed. Indexing of the PXRD

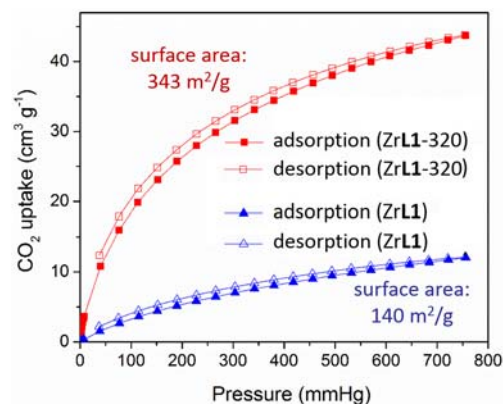


**Fig. 4.** CO<sub>2</sub> (273 K) adsorption and desorption isotherms for an activated ZrL1 crystal sample (blue graphs) and ZrL1-320 (i.e., after being heated at 320 °C) (red graphs).

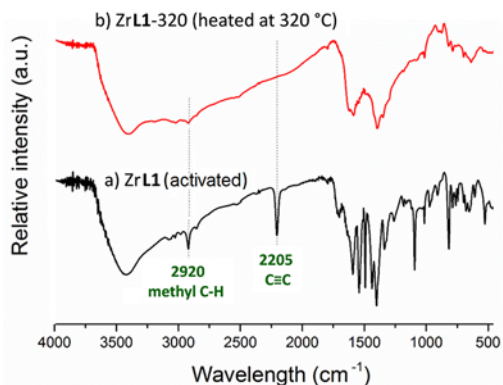


**Fig. 5.** IR spectra for (a) activated ZrL1; (b) ZrL1-320, i.e., activated ZrL1 heated at 320 °C for 3 hours.

peaks of the ZrL1-320 (i.e., the 320 °C-treated sample; pattern e of Fig. 3) reveals a tetragonal lattice with  $a = 21.35$ ,  $c = 29.41$  Å; with diffuse reflectance indicating a bandgap of 0.82 eV (Fig. S5). Even though N<sub>2</sub> uptake was not significant for the ZrL1-ac and ZrL1-320 samples thus obtained, CO<sub>2</sub> gas sorption indicated a substantial increase of surface area: from a Langmuir surface area of 140 m<sup>2</sup>/g for the activated ZrL1-ac to 343 m<sup>2</sup>/g for ZrL1-320 (Fig. 4 and S6).

The drastic chemical transformations from the thermal treatment are also seen in the IR spectra, with the distinct alkyne stretching at 2205 cm<sup>-1</sup> of ZrL1 completely vanished in the ZrL1-320 sample (Fig. 5). In addition, the C-H 2920 cm<sup>-1</sup> associated with the CH<sub>3</sub>S-groups of as-made ZrL1 was also greatly diminished in ZrL1-320, indicating the cleavage of the CH<sub>3</sub>-S bond (e.g., to form aryl-S-aryl bonds, emitting CH<sub>3</sub>SCH<sub>3</sub> and CH<sub>3</sub>SH; see also the illustration in Fig. 2). To further characterize the emitted molecules, a sample of ZrL1-ac heated in a sealed tube at 320 °C for 3 hours, and CDCl<sub>3</sub> was then added to collect the soluble products for NMR analysis. A comparison with standard samples of CH<sub>3</sub>SCH<sub>3</sub> and CH<sub>3</sub>SH (Fig. S7) confirms the formation of these molecules in the thermocyclization process (see Fig. S8 for a proposed mechanism). The departure of these sulfur-rich molecules is also reflected in the considerable weight loss at 320 °C revealed by TGA studies (Fig. S8), and in the decreased S/Zr molar ratios (2.38/1 in ZrL1-320, and 3.85/1 in ZrL1) semi-quantitatively measured by EDX (Fig. S9).

Solid-state <sup>13</sup>C NMR measurement on the ZrL1-320 sample also verifies the efficient benzannulation reaction. As seen in Fig. S10, the spectrum is dominated by two broad signals at the aromatic region (the principal one at 128 ppm with a shoulder at 137 ppm). The latter signal (around 137 ppm) most likely arises from the two C-S carbons and the 16 edge quaternary carbons (as marked in the inset), since these have been found to shift to relatively low field in polycyclic aromatics;<sup>11</sup> the main peak at 128 ppm can be assigned to the remaining aromatic C atoms (total number: 32). The peak of the two carboxyl carbons, generally occurring between 170-180 ppm, is not distinct because of their small number and consequently weak signal. The overall peak profile also compares well with those of a graphene nanoribbon made from thermally aromatizing an aryl diacetylene precursor.<sup>12</sup> Electrical conductivity measurements help to reveal significant  $\pi$ -conjugation and electron delocalization in the ZrL1-320. In a preliminary two-probe measurement, the thermocyclized sample ZrL1-320 (compressed powder), upon doped by Br<sub>2</sub>, exhibits a conductivity on the order of 10<sup>-2</sup> S/m. We are experimenting with the thermal treatment conditions, in order to optimize the performance of the resulted sample in electronic conductivity and other properties.

Remarkably, the thermally treated crystals (i.e., ZrL1-320) exhibit extraordinary stability against acids and bases. For example, whereas the F<sup>-</sup> ion and phosphoric acid (H<sub>3</sub>PO<sub>4</sub>) have proven especially detrimental to Zr(IV)-carboxylate networks (because of the stability of zirconium phosphate and fluoride compounds),<sup>13</sup> the ZrL1-320 crystals continue to feature strong and well-defined PXRD peaks consistent with the original lattice, even after being immersed in either 10% (w/w) H<sub>3</sub>PO<sub>4</sub> or in saturated NaF solutions (4% w/w, heated to 50 °C) for 24 hours, as is shown in patterns f and g of Fig. 3).

The above results (especially the stability and conductivity results) thus indicate that extensive cyclization and crosslinking across the linker molecules have been successfully induced by thermally treating the Zr-L1 scaffold (e.g., at 320 °C). The retention of the structural integrity of the Zr-L1 scaffold is clearly indicated by the PXRD analysis and the gas sorption studies. We are now building on this encouraging discovery and aiming to achieve more versatile functions and porosity properties in crystalline frameworks derived from tailor-made backfolded aromatic building blocks.

## ASSOCIATED CONTENT

### Supporting Information

Experimental procedure and additional data, including NMR spectra, the TGA plot, CO<sub>2</sub> sorption isotherms and PXRD refinement details. This material is available free of charge via the Internet at <http://pubs.acs.org>.

## AUTHOR INFORMATION

### Corresponding Author

\*zhengtao@cityu.edu.hk.

## ACKNOWLEDGMENT

This work is supported by the Research Grants Council of the Hong Kong Special Administrative Region [Project No. 11305915] and a CityU Internal Grant (SRG-fd 7004653) and Science and Technology Planning Project of Guangdong Province (2017A050506051).

## Notes and references

1. a) M. Maruyama and S. Okada, *Appl. Phys. Express*, 2013, **6**, 095101/1; b) R. Lv, E. Cruz-Silva and M. Terrones, *ACS Nano*, 2014, **8**, 4061; c) H. Terrones, F. Lopez-Urias, E. Munoz-Sandoval, J. A. Rodriguez-Manzo, A. Zamudio, A. L. Elias and M. Terrones, *Solid State Sci.*, 2006, **8**, 303; d) B. Wang, X. Wang, J. Zou, Y. Yan, S. Xie, G. Hu, Y. Li and A. Dong, *Nano Lett.*, 2017, **17**, 2003; e) K. Kim, T. Lee, Y. Kwon, Y. Seo, J. Song, J. K. Park, H. Lee, J. Y. Park, H. Ihee, S. J. Cho and R. Ryoo, *Nature* 2016, **535**, 131; f) K. Nueangnoraj, H. Nishihara, K. Imai, H. Itoi, T. Ishii, M. Kiguchi, Y. Sato, M. Terauchi and T. Kyotani, *Carbon*, 2013, **62**, 455; g) R. Zhou, R. Liu, L. Li, X. Wu and X. C. Zeng, *J. Phys. Chem. C*, 2011, **115**, 18174.
2. a) H. Terrones and A. L. Mackay, *Nature* 1991, **352**, 762; b) M. O'Keeffe, G. B. Adams and O. F. Sankey, *Phys. Rev. Lett.*, 1992, **68**, 2325.
3. a) T. Lenosky, X. Gonze, M. Teter and V. Elser, *Nature* 1992, **355**, 333; b) M. Tagami, Y. Liang, H. Naito, Y. Kawazoe and M. Kotani, *Carbon*, 2014, **76**, 266; c) H. Weng, Y. Liang, Q. Xu, R. Yu, Z. Fang, X. Dai and Y. Kawazoe, *Phys. Rev. B*, 2015, **92**, 1; d)

- A. Lherbier, H. Terrones and J.-C. Charlier, *Phys. Rev. B*, 2014, **90**, 125434/1; e) B. Szeffler, O. Ponta and M. V. Diudea, *J. Mol. Struct.*, 2012, **1022**, 89; f) D. Odkhuu, D. H. Jung, H. Lee, S. S. Han, S.-H. Choi, R. S. Ruoff and N. Park, *Carbon*, 2014, **66**, 39.
4. a) B. F. Hoskins and R. Robson, *J. Am. Chem. Soc.*, 1989, **111**, 5962; b) S. S. Y. Chui, S. M. F. Lo, J. P. H. Charmant, A. G. Orpen and I. D. Williams, *Science*, 1999, **283**, 1148; c) G. B. Gardner, D. Venkataraman, J. S. Moore and S. Lee, *Nature* 1995, **374**, 792; d) O. M. Yaghi, G. M. Li and H. L. Li, *Nature*, 1995, **378**, 703; e) K. M. Thomas, *Dalton Trans.*, 2009, 1487; f) G. Férey, *Chem. Soc. Rev.*, 2008, **37**, 191; g) R. Robson, *Dalton Trans.*, 2008, 5113; h) S. Kitagawa and R. Matsuda, *Coord. Chem. Rev.*, 2007, **251**, 2490; i) D. Bradshaw, J. B. Claridge, E. J. Cussen, T. J. Prior and M. J. Rosseinsky, *Acc. Chem. Res.*, 2005, **38**, 273; j) S. Lee, A. B. Mallik, Z. Xu, E. B. Lobkovsky and L. Tran, *Acc. Chem. Res.*, 2005, **38**, 251; k) N. W. Ockwig, O. Delgado-Friedrichs, M. O'Keeffe and O. M. Yaghi, *Acc. Chem. Res.*, 2005, **38**, 176; l) K. S. Suslick, P. Bhyrappa, J. H. Chou, M. E. Kosal, S. Nakagaki, D. W. Smithenry and S. R. Wilson, *Acc. Chem. Res.*, 2005, **38**, 283; m) Z. Xu, *Coord. Chem. Rev.*, 2006, **250**, 2745; n) D. Zhao, D. J. Timmons, D. Yuan and H.-C. Zhou, *Acc. Chem. Res.*, 2011, **44**, 123; o) S. M. Cohen, *Chem. Rev.*, 2012, **112**, 970; p) Y. Liu, W. Xuan, H. Zhang and Y. Cui, *Inorg. Chem.*, 2009, **48**, 10018; q) T. J. Morin, A. Merkel, S. V. Lindeman and J. R. Gardinier, *Inorg. Chem.*, 2010, **49**, 7992; r) S. Dawn, S. R. Salpage, M. D. Smith, S. K. Sharma and L. S. Shimizu, *Inorg. Chem. Commun.*, 2012, **15**, 88; s) K. Roy, M. D. Smith and L. S. Shimizu, *Inorg. Chim. Acta*, 2011, **376**, 598; t) M. H. Mir, L. L. Koh, G. K. Tan and J. J. Vittal, *Angew. Chem., Int. Ed.*, 2010, **49**, 390; u) W. L. Leong and J. J. Vittal, *Chem. Rev.*, 2011, **111**, 688; v) T. C. W. Mak, X.-L. Zhao, Q.-M. Wang and G.-C. Guo, *Coord. Chem. Rev.*, 2007, **251**, 2311.
  5. a) Q. Sun, B. Aguila, J. Perman, L. D. Earl, C. W. Abney, Y. Cheng, H. Wei, N. Nguyen, L. Wojtas and S. Ma, *J. Am. Chem. Soc.*, 2017, **139**, 2786; b) X. Wang, X. Han, J. Zhang, X. Wu, Y. Liu and Y. Cui, *J. Am. Chem. Soc.*, 2016, **138**, 12332; c) N. Huang, L. Zhai, H. Xu and D. Jiang, *J. Am. Chem. Soc.*, 2017, **139**, 2428; d) H. Li, Q. Pan, Y. Ma, X. Guan, M. Xue, Q. Fang, Y. Yan, V. Valtchev and S. Qiu, *J. Am. Chem. Soc.*, 2016, **138**, 14783; e) Q. Fang, J. Wang, S. Gu, R. B. Kaspar, Z. Zhuang, J. Zheng, H. Guo, S. Qiu and Y. Yan, *J. Am. Chem. Soc.*, 2015, **137**, 8352; f) A. Nagai, X. Chen, X. Feng, X. Ding, Z. Guo and D. Jiang, *Angew. Chem., Int. Ed.*, 2013, **52**, 3770; g) D. N. Bunck and W. R. Dichtel, *Angew. Chem., Int. Ed.*, 2012, **51**, 1885; h) A. P. Cote, A. I. Benin, N. W. Ockwig, M. O'Keeffe, A. J. Matzger and O. M. Yaghi, *Science*, 2005, **310**, 1166; i) Q. Fang, Z. Zhuang, S. Gu, R. B. Kaspar, J. Zheng, J. Wang, S. Qiu and Y. Yan, *Nat. Commun.*, 2014, **5**, 4503pp; j) S. Das, P. Heasman, T. Ben and S. Qiu, *Chem. Rev.*, 2017, **117**, 1515; k) C. R. DeBlase and W. R. Dichtel, *Macromolecules* 2016, **49**, 5297; l) P. Kuhn, M. Antonietti and A. Thomas, *Angew. Chem., Int. Ed.*, 2008, **47**, 3450; m) K. Sakaushi and M. Antonietti, *Acc. Chem. Res.*, 2015, **48**, 1591; n) G. Lin, H. Ding, R. Chen, Z. Peng, B. Wang and C. Wang, *J. Am. Chem. Soc.*, 2017, **139**, 8705.
  6. a) Z. Xu, S. Lee, Y.-H. Kiang, A. B. Mallik, N. Tsomaia and K. T. Mueller, *Adv. Mater.*, 2001, **13**, 637; b) Y.-H. Kiang, G. B. Gardner, S. Lee and Z. Xu, *J. Am. Chem. Soc.*, 2000, **122**, 6871; c) K.-K. Yee, N. Reimer, J. Liu, S.-Y. Cheng, S.-M. Yiu, J. Weber, N. Stock and Z. Xu, *J. Am. Chem. Soc.*, 2013, **135**, 7795; d) J. He, M. Zeller, A. D. Hunter and Z. Xu, *CrystEngComm*, 2015, **17**, 9254; e) T. Ishiwata, Y. Furukawa, K. Sugikawa, K. Kokado and K. Sada, *J. Am. Chem. Soc.*, 2013, **135**, 5427.
  7. a) C. Yang, Y.-L. Wong, R. Xiao, M. Zeller, A. D. Hunter, S.-M. Yiu and Z. Xu, *ChemistrySelect*, 2016, **1**, 4075; b) J. Cui, Y.-L. Wong, M. Zeller, A. D. Hunter and Z. Xu, *Angew. Chem., Int. Ed.*, 2014, **53**, 14438; c) Y.-Q. Sun, C. Yang, Z. Xu, M. Zeller and A. D. Hunter, *Cryst. Growth Des.*, 2009, **9**, 1663; d) Y.-Q. Sun, J. He, Z. Xu, G. Huang, X.-P. Zhou, M. Zeller and A. D. Hunter, *Chem. Commun.*, 2007, 4779; e) Z. Xu, Y.-Q. Sun, J. He, M. Zeller and A. D. Hunter, in *The concept and use of a class of branchy molecules with centripetal self-similarity*, Nova Science Publishers, Inc., Hauppauge, NY 2008; f) W. Yang, G. Longhi, S. Abbate, A. Lucotti, M. Tommasini, C. Villani, V. J. Catalano, A. O. Lykhin, S. A. Varganov and W. A. Chalifoux, *J. Am. Chem. Soc.*, 2017, **139**, 13102; g) R. Nandy, M. Subramoni, B. Varghese and S. Sankararaman, *J. Org. Chem.*, 2007, **72**, 938.
  8. a) K. Kongpatpanich, S. Horike, Y.-i. Fujiwara, N. Ogiwara, H. Nishihara and S. Kitagawa, *Chem. - Eur. J.*, 2015, **21**, 13278; b) J.-K. Sun and Q. Xu, *Energy Environ. Sci.*, 2014, **7**, 2071; c) A. Aijaz, N. Fujiwara and Q. Xu, *J. Am. Chem. Soc.*, 2014, **136**, 6790; d) W. Chaikittisilp, K. Ariga and Y. Yamauchi, *J. Mater. Chem. A*, 2013, **1**, 14; e) S. J. Yang, T. Kim, J. H. Im, Y. S. Kim, K. Lee, H. Jung and C. R. Park, *Chem. Mater.*, 2012, **24**, 464; f) J. Hu, H. Wang, Q. Gao and H. Guo, *Carbon*, 2010, **48**, 3599; g) B. Liu, H. Shioyama, T. Akita and Q. Xu, *J. Am. Chem. Soc.*, 2008, **130**, 5390; h) C. Liang, Z. Li and S. Dai, *Angew. Chem., Int. Ed.*, 2008, **47**, 3696; i) K. Xi, S. Cao, X. Peng, C. Ducati, R. V. Kumar and A. K. Cheetham, *Chem. Commun.*, 2013, **49**, 2192.
  9. M. Carboni, Z. Lin, C. W. Abney, T. Zhang and W. Lin, *Chem. - Eur. J.*, 2014, **20**, 14965.
  10. S. Yuan, W. Lu, Y.-P. Chen, Q. Zhang, T.-F. Liu, D. Feng, X. Wang, J. Qin and H.-C. Zhou, *J. Am. Chem. Soc.*, 2015, **137**, 3177.
  11. T. Thonhauser, D. Ceresoli and N. Marzari, *Int. J. Quantum Chem.*, 2009, **109**, 3336.
  12. R. S. Jordan, Y. L. Li, C.-W. Lin, R. D. McCurdy, J. B. Lin, J. L. Brosmer, K. L. Marsh, S. I. Khan, K. N. Houk, R. B. Kaner and Y. Rubin, *J. Am. Chem. Soc.*, 2017, **139**, 15878.
  13. a) C. W. Abney, K. M. L. Taylor-Pashow, S. R. Russell, Y. Chen, R. Samantaray, J. V. Lockard and W. Lin, *Chem. Mater.*, 2014, **26**, 5231; b) *Application: EP Pat.*, 3254755, 2017; c) Y.-L. Hou, K.-K. Yee, Y.-L. Wong, M. Zha, J. He, M. Zeller, A. D. Hunter, K. Yang and Z. Xu, *J. Am. Chem. Soc.*, 2016, **138**, 14852.

